

RESEARCH ARTICLE

Carbon exchange and primary production in a High-Arctic peatland in Svalbard

Takayuki Nakatsubo,^{1,2} Mitsuru Hirota,³ Ayaka W. Kishimoto-Mo,⁴ Noriko Oura⁴ & Masaki Uchida^{5,6}¹Graduate School of Integrated Sciences for Life, Hiroshima University, Higashi-Hiroshima, Japan²Hiroshima University Museum, Higashi-Hiroshima, Japan³School of Life and Environmental Science, University of Tsukuba, Tsukuba, Japan⁴Institute for Agro-Environmental Sciences, National Agriculture and Food Research Organization, Tsukuba, Japan⁵National Institute of Polar Research, Tachikawa, Japan⁶School of Multidisciplinary Sciences, The Graduate University for Advanced Studies, Tachikawa, Japan

Abstract

Moss tundra with a thick peat layer dominated by bryophytes is one of the most important ecosystems in the High Arctic of Svalbard, but little is known about the carbon dynamics of moss tundra. Here, we estimated the net primary production (NPP) and net ecosystem production (NEP) of moss tundra on Brøggerhalvøya (Brøgger Peninsula) of north-western Svalbard (79°N). The net photosynthetic and respiration rates of the two dominant moss species, *Calliergon richardsonii* and *Tomenthypnum nitens*, were measured under laboratory conditions. On the basis of the photosynthetic and respiration characteristics and climatic data, we estimated the cumulative NPP of the dominant moss species during the growing season to be 143–207 gC m⁻². Net CO₂ exchange, which was determined by subtracting the respiration of the brown moss layer from NPP, was similar to that estimated using field gas flux measurements. The field measurements indicated that methane emissions contributed little to carbon flow. The NEP estimated in this study was much larger than the long-term carbon accumulation rate reported in a previous study. These data suggest that a significant amount of fixed carbon was lost from the peat layer or that carbon accumulation has recently increased. The NPP and NEP values of the moss tundra are larger than those reported for other vegetation types in this area, suggesting that moss tundra is an active site with high rates of carbon fixation.

Keywords

Carbon flow; moss tundra; photosynthesis; respiration; *Calliergon richardsonii*; *Tomenthypnum nitens*

Abbreviations

BP: Before Present (0 cal BP = AD 1950)
NEP: net ecosystem production
NPP: net primary production
ORP: oxidation-reduction potential
PPFD: photosynthetic photon flux density
PVC: polyvinyl chloride

Correspondence

Takayuki Nakatsubo, Graduate School of Integrated Sciences for Life, Hiroshima University, Higashi-Hiroshima, 739-8521, Japan. E-mail: kuyakat@hiroshima-u.ac.jp

To access the supplementary material, please visit the article landing page

Introduction

Northern peatlands represent one of the largest carbon pools in the biosphere and play a key role in the global carbon cycle (Yu 2012). The recent increase in temperature in Arctic regions, which is more than twice the global rate over the past 50 years (IPCC 2021), is likely to have a profound influence on the carbon pool by altering the balance between carbon accumulation and loss.

Carbon pools in the High Arctic are likely small because of the harsh climatic conditions and lack of plant cover; however, a non-negligible amount of carbon exists

in soils in areas at late successional stages (Yoshitake et al. 2011). Several studies have shown that there is a large amount of organic carbon in High-Arctic moss tundra, which comprises moss-dominated wetlands with a thick peat layer. For example, Rozema et al. (2006) reported 1-m thick peat layers dating back maximally to 5710 ± 150 BP from the moss tundra in Svalbard. Nakatsubo et al. (2015) estimated that 276 tonnes of organic carbon are stored in the active layer of a 40 000-m² area (6.9 kgC m⁻²) of moss tundra in Svalbard. Because the carbon budget of moss tundra is determined by the balance between carbon accumulation and loss, analyses of

these flows and the factors controlling them are needed to predict the impact of climate change on the carbon cycle in High-Arctic ecosystems. However, data on the carbon flows in High-Arctic peatlands are few.

The aim of this study was to clarify the carbon dynamics of moss tundra, which is peatland characterized by a thick peat-forming community dominated by bryophytes (Vanderpuyé et al. 2002), in the High Arctic of Svalbard. We measured the photosynthetic characteristics of dominant moss species and the respiration of the active layer (brown moss layer) under laboratory conditions. We then modelled the NPP and NEP (the difference between gross primary production and total ecosystem respiration) for the growing season, using the measured photosynthetic and respiration characteristics and climatic data. It is likely that the NPP and NEP show considerable year-to-year variation, depending on climatic conditions that include the length of growing season. Therefore, we calculated the values for three seasons using climatic data from 2012 to 2014. Additionally, we measured the methane (CH_4) flux at the same site and estimated the CH_4 flux during the growing season because it is one of the main degradation pathways of plant polymers in High-Arctic peatlands (Tveit et al. 2013).

Methods

Study site

The study site, Stuphallet, is located in the northern part of Brøggerhalvøya (Brøgger Peninsula), near Ny-Ålesund, north-western Spitsbergen, Svalbard (78°57'N, 11°39–40'E, 22 m a.s.l.). With a maximum width of 100 m, a swathe of moss tundra, runs along two streams: one flowing from east to west and the other from west to east between a bank and a bird-nesting cliff. The annual mean air temperature and precipitation between 2011 and 2020 in Ny-Ålesund, which is located approximately 7 km from the study site, were -2.9 °C and 550 mm, respectively (Yr 2021).

The study site was completely covered with a thick peat layer dominated by moss species such as *Calliergon richardsonii* (Mitt.) Kindb., *Tomenthypnum nitens* (Hedw.) Loeske, *Paludella squarrosa* Bridel, and *Warnstorfia exannulata* (Schimp.) Loeske. The average thickness of the active layer (brown moss and peat) in early August 2011 was approximately 28 cm. See Nakatsubo et al. (2015) for a detailed description of the study site.

Sample collection

Moss samples were collected from two dominant moss species, *C. richardsonii* and *T. nitens*, on the basis of a

preliminary field survey. The samples were collected from colonies using a metal core sampler with a diameter of 5 cm in the summers of 2013 and 2015. Moss cores were divided into three layers: a green (surface) layer consisting of green shoots (20–29 mm thick), a brown sub-surface layer consisting of brown shoots (40–64 mm thick) and a peat layer consisting of fragmented shoots. Most of the peat layer was under the water table (waterlogged). Samples of the green and brown layers were immediately brought to the laboratory in Ny-Ålesund and placed in cylindrical plastic cases (\varnothing : 5 cm, height: 10 cm). They were then stored in an incubator at 5 °C under continuous light after taking fresh weight measurements. During measurements, the water content of the moss samples was maintained at 330–390% (w/w), which corresponds to the water content of moss under field conditions at our study site.

Photosynthesis and respiration measurements

We measured the net photosynthetic rate (P_n), dark respiration (R) of the green moss layer, and dark respiration of the brown moss layer (R_b) using an open-flow gas exchange system with a Li-Cor Biosciences infrared gas analyser (model LI-6262). Uchida et al. (2002) described the system in detail. We placed a plastic case containing the sample into a cylindrical transparent chamber (\varnothing : 7 cm, height: 4 cm). The chamber was submerged in a water bath with a temperature control unit to maintain target temperatures within an accuracy of $\pm 0.2\text{ °C}$. Ambient air containing 390–400 ppmv CO_2 was introduced into the system at a rate of 300 ml min^{-1} , and a Hayashi Tokei Kogyo 180-W metal halide lamp (model LA-180Me) supplied light. Unless otherwise noted, the temperature in the chamber and PPFD were maintained at $7.0 \pm 0.2\text{ °C}$ and $1500 \pm 30\ \mu\text{mol photons m}^{-2}\text{ s}^{-1}$, respectively.

The effect of PPFD on P_n was determined by reducing the incident PPFD on the chamber. Samples ($n = 6$) were illuminated at each level of PPFD for at least three minutes before P_n was measured.

To examine the effect of temperature on P_n and R , the moss temperature in the chamber was reduced in a step-wise manner from 23 to 2 °C at 5–6 °C intervals ($n = 6$). The temperature was maintained at each step for at least 30 minutes to allow gas exchange rates to stabilize. After measurements were taken, the samples were freeze-dried for dry weight determination. The effect of temperature on R_b (dark respiration of the brown moss layer) was also measured in the same manner described here ($n = 10$).

Estimation of moss production

We estimated the NPP and NEP on the basis of the photosynthesis and respiration characteristics and climatic data.

At our study site, site-to-site variation in species composition was considerable. Given the difficulty of determining the relative abundance of each species across the entire study area, we used the average values of the photosynthetic and respiration characteristics of the two species to estimate NPP and NEP values (Table 1).

NPP of mosses was estimated using a slightly modified version of the model described by Nakatsubo (2002), who examined the environmental dependence of photosynthetic production. Here, we assumed that the moss water content did not affect photosynthetic and respiration activities because water was supplied continuously on the moss tundra. The water content of the mosses was consistently high ($701 \pm 237\%$ for *C. richardsonii* and $398 \pm 106\%$ for *T. nitens*) during in situ gas exchange measurements taken from 8 Jul to 9 Aug 2013. We also assumed that the main environmental factors affecting NPP are light and temperature (Harley et al. 1989; Froelking et al. 2002; Uchida et al. 2002). All moss samples were exposed to standard light and temperature conditions (light saturation at PPFD = $1500 \mu\text{mol m}^{-2} \text{s}^{-1}$ and 7°C , respectively).

$$P_g(T) = P_n(T) + R(T) \quad (1)$$

$$P_n(T) = P_n(7) \times (aT^2 + bT + c) \quad (2)$$

$$R(T) = R(7) \times Q_{10}^{(T-7)/10} \quad (3)$$

$$P_g(I) = P_g(7)(1 - e^{-SI}) \quad (4)$$

$$P_g(I, T) = P_g(I) \times P_g(T) / P_g(7) \quad (5)$$

$$P_n(I, T) = P_g(I, T) - R(T) \quad (6)$$

$$NPP_w = \Sigma P_n(I, T), \quad (7)$$

where $P_g(T)$ is the gross photosynthetic rate at light saturation and $T^\circ\text{C}$ ($\text{mgCO}_2\text{-C g}^{-1} \text{h}^{-1}$); $P_n(T)$ is the net photosynthetic rate at light saturation and $T^\circ\text{C}$; $R(T)$ is the respiration rate at $T^\circ\text{C}$; Q_{10} (an indicator of temperature sensitivity) is shown for the green moss layer; $P_g(I, T)$ and $P_n(I, T)$ are the gross and net photosynthetic rate at $I \mu\text{mol m}^{-2} \text{s}^{-1}$ PPFD and $T^\circ\text{C}$ ($\text{mgCO}_2\text{-C g}^{-1} \text{h}^{-1}$), respectively; and $P_g(7)$, $P_n(7)$, and $R(7)$ are P_g , P_n , and R at 7°C , respectively. a , b and c are the coefficients of the temperature-photosynthetic curve; S is the coefficient of the light-photosynthetic curve; and NPP_w (gC g^{-1}) is the cumulative NPP during the growing season.

The effect of temperature (T_B) on the respiration of the brown moss layer (R_B) was determined using Eqn. 8.

$$R_B(T_B) = R_B(7) \times Q_{10B}^{(T_B-7)/10}, \quad (8)$$

Table 1 Coefficients and standard values used for the model for the estimation of the green layer and brown layer.

Coefficients and standard values	<i>Calliergon richardsonii</i>	<i>Tomenthypnum nitens</i>	Average
Green layer			
a^a	-0.0017	-0.0009	-0.0014
b^a	0.0257	0.0133	0.0214
c^a	0.8052	0.9117	0.8419
S^b	0.0051	0.0087	0.0061
$P_n(7)$	0.7863	0.4139	0.6001
$R(7)$	0.1680	0.0616	0.1148
$P_g(7)$	0.9543	0.4755	0.7149
Q_{10}^c	2.4	2.3	2.4
Brown layer			
$R_B(7)$	0.0456	0.0202	0.0329
Q_{10B}^d	2.2	2.4	2.2

^aCoefficients of the temperature-photosynthetic curve (Eqn. 2). ^bThe coefficient of the light-photosynthetic curve (Eqn. 4). ^cAn indicator of the temperature sensitivity of the respiration rate of the green layer (Eqn. 3). ^dAn indicator of the temperature sensitivity of the respiration of the brown layer (Eqn. 8).

where $R_B(7)$ is R_B at 7°C , and Q_{10B} is the Q_{10} of respiration of the brown moss layer.

Finally, the NEP during the growing season (NEP_w ; $\text{gCO}_2\text{-C g}^{-1}$) was calculated as follows:

$$NEP_w = \Sigma(P_n(I, T) - R_B(T_B)) \quad (9)$$

NPP and NEP during the growing season were converted from a dry weight basis ($\text{gCO}_2\text{-C g}^{-1}$) to an areal basis (NPP and NEP; $\text{gCO}_2\text{-C m}^{-2}$) using the average weights of the green moss layer ($287 \text{ g dry wt. m}^{-2}$) and average weights of the brown moss layer ($1582 \text{ g dry wt. m}^{-2}$).

Hourly PPFD and temperature data of the green and brown moss layer from 2012 to 2014 were used to estimate NEP. PPFD was measured using a KONA System data logger (model Kadec-UP) with a Li-Cor quantum sensor (model Li-190SA) placed at the Japanese base in Ny-Ålesund. Temperatures in the green (2 cm below the moss surface) and brown (5 cm below the moss surface) moss layers were measured using Hobo temperature data loggers (model Tidbit v2) placed in the moss tundra. The growing season was defined as the period when the temperature of the moss layers was above 0°C .

In situ gas exchange measurements

Net CO_2 exchange was determined in the field from 8 Jul to 9 Aug 2013 using the static closed-chamber method described by Hirota et al. (2010). We established four plots every 20 m along an 80-m transect across the moss

tundra, in accordance with the method used by Nakatsubo et al. (2015) and placed three PVC collars 2 cm into the ground in the moss tundra in each plot two days before measurements were initiated. Each of the collars in each plot was separated by more than 1 m. The chamber (20 cm in diameter and 12.5 cm in height), made of transparent PVC pipe with a top plate and open bottom, was placed on the collar just prior to the start of the in situ CO₂ exchange measurements. Net CO₂ exchange rates were determined by monitoring changes in the CO₂ concentration within the chamber with a Vaisala CO₂ probe (model GMP 343). During measurements, the PPF_D outside the chamber and temperature and humidity in the chamber were recorded. A small fan was placed in the chamber to mix (circulate) the air. We placed a black screen on the chamber to determine ecosystem respiration (R_E). The response of the gas exchange rate to light conditions was determined by decreasing the PPF_D using a translucent polyethylene sheet. It took approximately five to 15 minutes for the flux rates to stabilize during each measurement. Net CO₂ exchange rates for 8–12 plots were recorded each measurement day. All measurements were made between 11:00 and 19:00.

CH₄ flux was measured using a chamber of the same size and period. The chamber was made of opaque PVC without any sensors. We placed four chambers on the collar just prior to the measurements and took air (25 ml) into the chamber four times at 4–5-minute intervals. The air was collected into pre-evacuated glass vials and brought to Japan. We determined the CH₄ concentration using a Shimadzu gas chromatograph (model GC-14B) with a thermal conductivity detector and a flame ionization detector. Calibration of the GC-14B was conducted using two concentrations of CH₄ standards (1.254–2.013 ppmv). The CH₄ concentrations from each chamber were plotted against the sampling time, and the data were fitted with linear regression lines to determine changes in CH₄ concentrations ($R^2 \geq 0.90$). Hayashi et al. (2014) described the flux calculations in detail. While taking air samples, we measured the water table and ORP in each plot. PVC pipe (ϕ : 5 cm, length: 40 cm) with holes drilled in four directions (ϕ : 5 mm, every 3 cm) was installed in each plot two days before measurements. The water table in the pipe was observed. The ORP measurements were conducted using a Satotech portable Eh meter (model YK-23RP-ADV) by inserting the platinum electrode into the peat layer.

We cut the green part of the moss in the chambers after taking the final measurement on 9 Aug 2013, and the fresh weight and dry weight (after freeze-drying to constant weight) of these samples were determined in Ny-Ålesund.

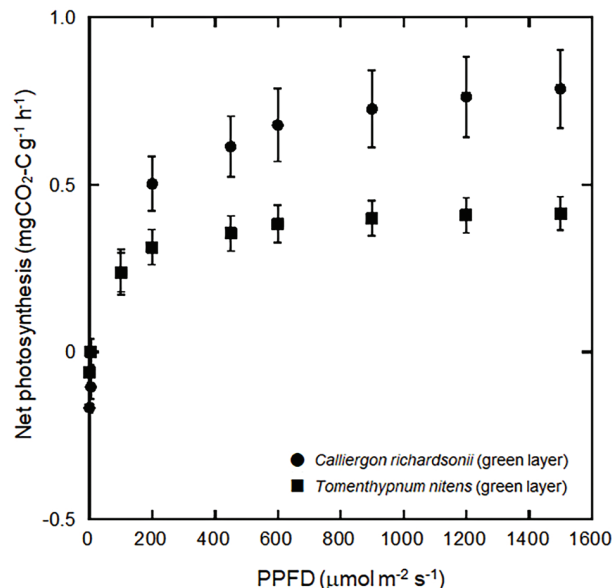


Fig. 1 Light-net photosynthesis curves of *Calliergon richardsonii* and *Tomenthypnum nitens*. Temperature: 7.0 ± 0.2 °C. Each value is the mean of three samples with SD.

Statistical analyses

All data were presented as mean \pm standard deviations unless otherwise specified. All statistical tests were performed using StatView 4.0 software (Abacus Concepts). We used standard statistical approaches for regression analysis to test the significance of the regression equations, and the significance of the relationships between gas exchange rates and environmental factors.

Results

Photosynthesis and respiration of mosses

The maximum P_n at light saturation (PPFD = $1500 \mu\text{mol m}^{-2} \text{s}^{-1}$) and 7 °C was higher in *C. richardsonii* ($0.8 \pm 0.1 \text{ mgCO}_2\text{-C g}^{-1} \text{h}^{-1}$) than in *T. nitens* ($0.4 \pm 0.05 \text{ mgCO}_2\text{-C g}^{-1} \text{h}^{-1}$) (Fig. 1). P_n of *C. richardsonii* at light saturation ($1500 \mu\text{mol m}^{-2} \text{s}^{-1}$) was highest at approximately 7 °C and decreased at 23 °C (Fig. 2). The optimum temperature for P_n of *T. nitens* was unclear; however, P_n was lower at high temperatures. Dark respiration rates of the green moss layer and the brown moss layer (Fig. 3) of the two species increased exponentially with temperature; Q_{10} values ranged from 2.2 to 2.4 (Table 1).

Gas exchange in the field

Net CO₂ exchange rates determined on the moss surface under natural light conditions ranged from -6 to 173

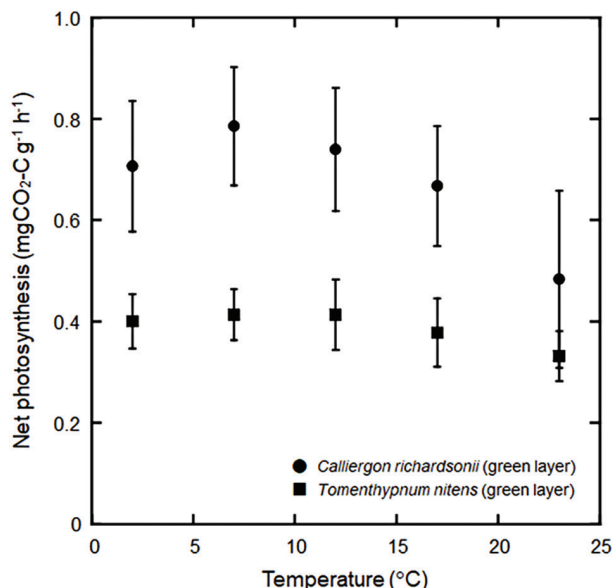


Fig. 2 Effect of temperature on the net photosynthetic rate of *Calliergon richardsonii* and *Tomenthypnum nitens*. PPFD: 1500 ± 30 μmol photons m⁻² s⁻¹. Each value is the mean of three samples with SD.

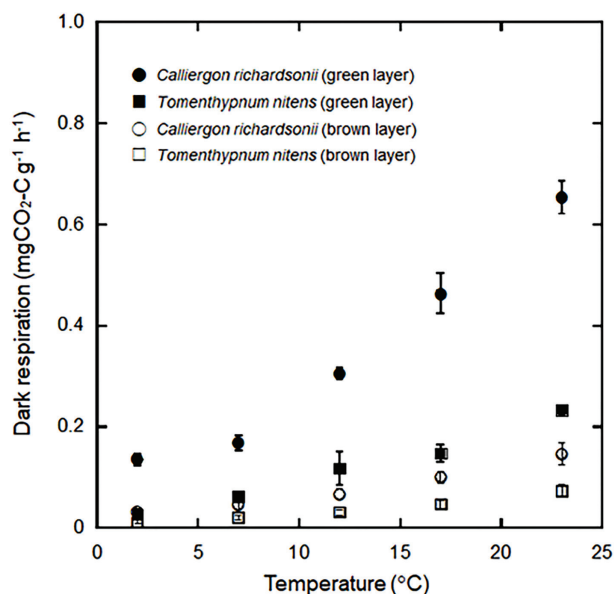


Fig. 3 Effect of temperature on the dark respiration rate of the green and brown moss layer of *Calliergon richardsonii* and *Tomenthypnum nitens*. Each value is the mean of three samples with SD.

mgCO₂-C m⁻² h⁻¹ (Fig. 4). NEP appeared to be regulated by natural light conditions (Fig. 5a); however, temperature conditions varied in the field. There was no clear relationship between air temperature and ecosystem respiration (Fig. 5b).

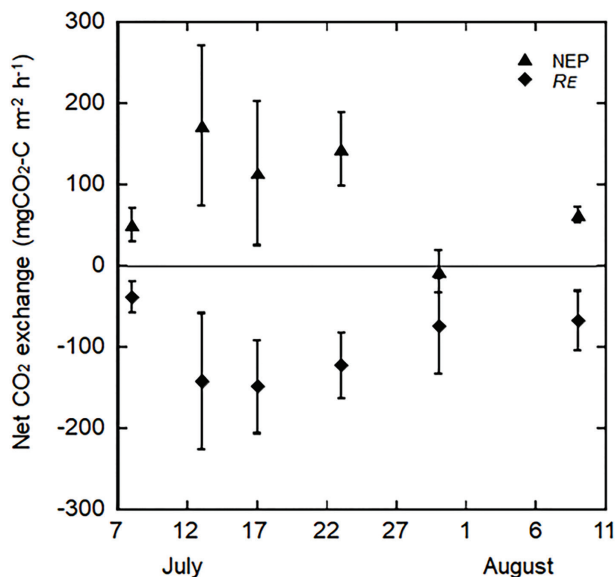


Fig. 4 NEP and ecosystem respiration (R_E) at the study site in summer 2013. Each value is the mean with SD ($n = 8-12$).

The CH₄ emission rates from the moss tundra were low and ranged from 9 to 65 μgCH₄-C m⁻² h⁻¹ (data not shown) (average: 34 μgCH₄-C m⁻² h⁻¹). There was no significant relationship between CH₄ flux and environmental factors such as temperature, water table and ORP ($p > 0.05$).

Estimation of NPP and NEP in the growing season

We estimated NEP values by subtracting the respiration of the brown moss layer from NPP values (Eqn. 9); we then compared them with the NEP values determined by gas flux measurements in the field (Fig. 6). For this comparison, NEP values under the artificially decreased light conditions were included. There was a significant relationship between the NEP values estimated by the model and those measured in the field. In addition, the slope of the regression line was close to 1, indicating that our model accurately estimated NEP in the field (Fig. 7).

We calculated NEP for three seasons using climatic data from 2012 to 2014 (Supplementary Fig. S1). In these calculations, we assumed that photosynthesis and respiration activities were negligible at temperatures lower than 0 °C. NPP and NEP values in 2012, 2013, and 2014 were estimated to be 205, 207 and 143 gC m⁻² and 88, 86 and 67 gC m⁻², respectively (Fig. 8). NPP and NEP values in 2012 and 2013 were similar, whereas NPP and NEP values in 2014 were lower than those in 2012 and 2013. Variation in the length of the growing season among sample years is the most likely explanation for these differences. Also, the growing degree days above 5 °C reflect

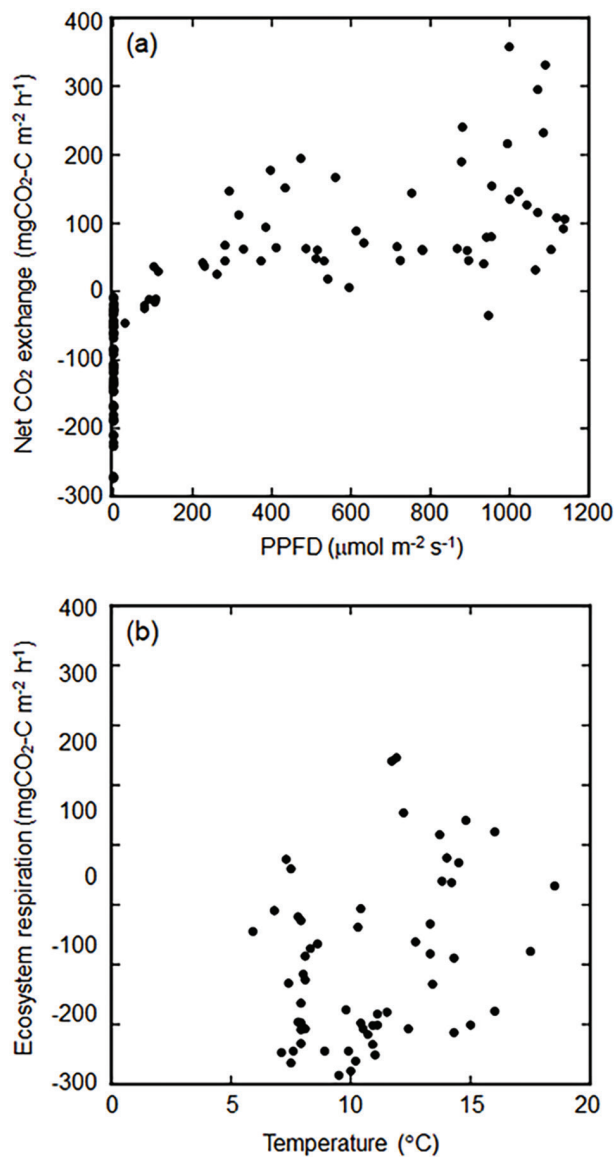


Fig. 5 (a) Effect of PPFD on the net CO₂ exchange and (b) the effect of air temperature on ecosystem respiration in the field in summer 2013.

the variation of the growing season length with values of 123, 140 and 57 in 2012–2014. The timing of snowmelt was delayed by over three weeks in 2014 compared with that in previous years (Supplementary Fig. S1b). Thus, the growing season in 2014 (75 days) was approximately two-thirds the length of the growing seasons in 2012 (104 days) and 2013 (110 days).

Discussion

NPP and NEP estimated by our model varied among three years (2012, 2013 and 2014), and the most marked

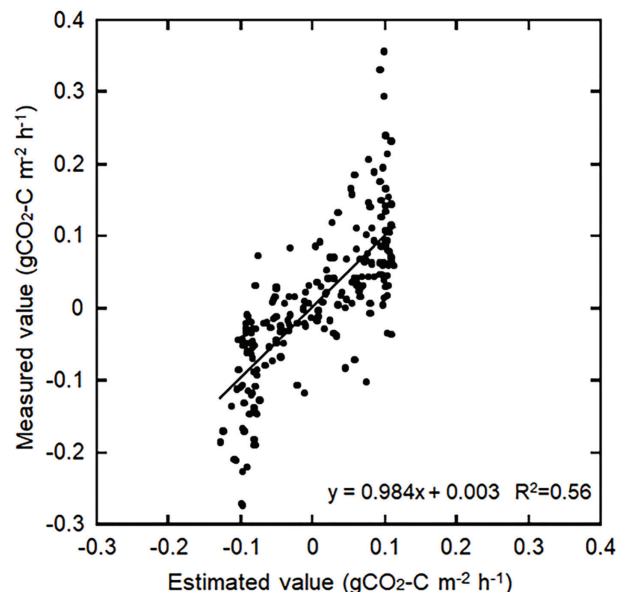


Fig. 6 Relationship between net CO₂ exchange values estimated by our model and those determined in the field in four study plots (A, B, C and D).

difference was in the NPP and NEP values of 2014, which were lower than those for 2012 and 2013. Previous studies (Uchida et al. 2002; Uchida et al. 2006; Yoshitake et al. 2010) have reported that the annual production of cryptogams (mosses, lichens, and the soil crust) in the High Arctic shows considerable year-to-year variation depending on climatic conditions.

P_n values at light saturation of the two tundra moss species (0.41–0.79 mgCO₂-C g⁻¹ h⁻¹) were similar to or somewhat higher than those reported for *Sanionia uncinata* (Hedw.) Loeske on a glacier foreland in Ny-Ålesund, Svalbard (0.45 ± 0.07 mgCO₂-C g⁻¹ h⁻¹) (Uchida et al. 2002). However, NPP of the moss tundra during the growing season estimated in this study (143–207 gC m⁻²) was much larger than the NPP of a *Sanionia* colony (100% moss coverage) on a glacier foreland (0.5–14 gC m⁻²; Uchida et al. 2002). The low NPP of *S. uncinata* can be largely explained by the low water availability on the glacier foreland because high photosynthetic activity has been observed only on rainy days or soon after rainfall (Uchida et al. 2002). The values of NPP estimated in this study were similar to or larger than those reported for *Calliergon stramineum* (Brid.) Kindb. in the tundra of Hornsund Fiord, Svalbard (77°00'N, 15°33'E), which were measured by a harvesting method (220–270 g dry weight m⁻² yr⁻¹; Opaliński 1991).

The NPP values of mosses were larger than the NPP values reported for other vegetation types in Svalbard. For example, during the growing season, the NPP of the polar willow (*Salix polaris* Wahlenb.), which has the

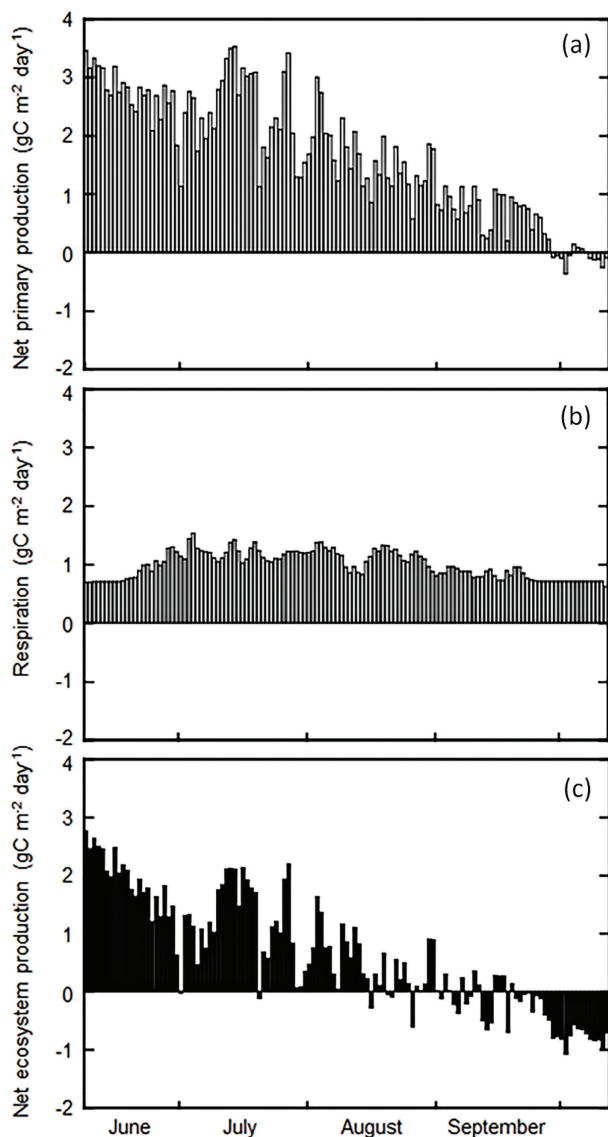


Fig. 7 (a) Daily NPP, (b) respiration of the brown moss layer, and (c) NEP in the growing season of 2013.

highest productivity among the vascular plants dominant on Svalbard's glacier forelands (Muraoka et al. 2008), was estimated to be 26.1 gC m^{-2} (53% plant cover; Muraoka et al. 2002). The higher NPP of mosses can be explained by differences in photosynthetic activity during the growing season; mosses are perennial evergreen plants that can photosynthesize in the autumn if water and light conditions are suitable for photosynthesis (Uchida et al. 2010). By contrast, the foliage period of *S. polaris* is much shorter (43 days) in this area (Muraoka et al. 2002).

Model estimates of productivity are prone to deviation caused by measurement errors, approximations,

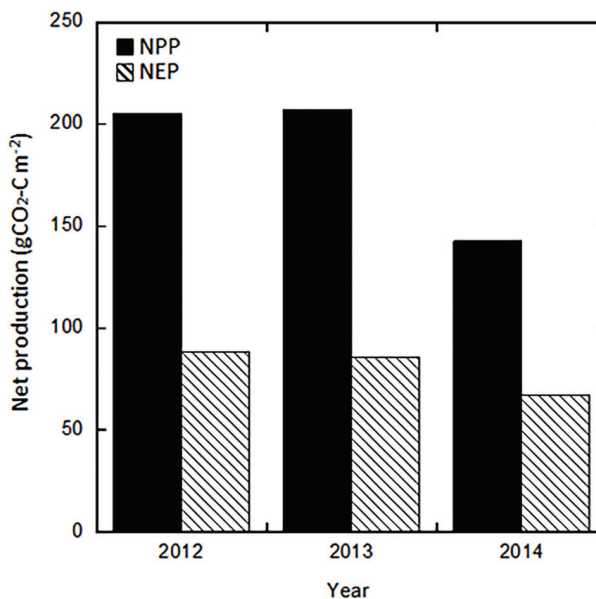


Fig. 8 Estimation of NPP and NEP in moss tundra during the growing season.

environmental fluctuations in the field, and differences between field and laboratory conditions. We estimated NEP by subtracting brown layer respiration from NPP. Because the CO_2 emissions of the peat layers were not included in this calculation, our NEP values might be slightly overestimated. However, there was a strong correlation between the NEP values estimated by our model and those measured in the field, indicating that the respiration of the peat layer was low. CO_2 emissions at sub-zero temperatures pose another difficulty in estimating NEP. In this study, the growing season was defined as the period when the temperature of the moss layers was above 0°C , assuming that photosynthesis and respiration at sub-zero temperatures were negligible. However, some studies have reported that the physiological activities of polar bryophytes continue at temperatures below 0°C (Longton 1988). Because light conditions in autumn and winter were insufficient for maintaining positive net photosynthesis (see Fig. 1, Supplementary Fig. S1), our assumption may have resulted in the overestimation of annual NEP. Positive NEP may be possible in the spring when more light is available; however, the carbon balance depends on the thickness of the snow cover.

Reported values of NEP in High-Arctic ecosystems vary widely (Table 2). NEP values in this study ($67\text{--}88 \text{ gC m}^{-2}$) were high but similar to those of a mixed dry and wet area in Longyearbyen, Svalbard (82 gC m^{-2} ; Pirk et al. 2017) and Lake Hazen, Ellesmere Island, Canada (79 gC m^{-2} ; Emmerton et al. 2016).

Table 2 NEP in the High Arctic.

Site	Latitude	Longitude	Habitat condition/ vegetation type	Dominant species	NEP (gC m ⁻² yr ⁻¹)	References
Ny-Ålesund, Svalbard	78°57'N	11°40'E	Moss tundra (wet)	<i>Calliergon richardsonii</i> , <i>Tomenthypnum nitens</i>	67 to 88 ^b	This study
Zackenbergl, Greenland	74°28'N	20°34'W	Heath	<i>Cassiope tetragona</i>	15	Zhang et al. 2018
Zackenbergl, Greenland	74°28'N	20°34'W	Heath	<i>Cassiope tetragona</i> , <i>Dryas integrifolia</i>	1 to 23 ^a	Groendahl et al. 2007
Alexandra Fiord, Canada	78°54'N	75°55'W	Dry	<i>Salix arctica</i> , <i>Dryas integrifolia</i>	6	Welker et al. 2004
Alexandra Fiord, Canada	78°54'N	75°55'W	Mesic	<i>Cassiope tetragona</i> , <i>Dryas integrifolia</i>	-18	Welker et al. 2004
Alexandra Fiord, Canada	78°54'N	75°55'W	Wet	<i>Eriophorum angustifolium</i> , <i>Carex stans</i>	15	Welker et al. 2004
Lake Hazen, Canada	81°08'N	71°04'W	Polar semi-desert upland (dry)	<i>Dryas integrifolia</i> , <i>Carex nardina</i>	0 ^b	Emmerton et al. 2016
Lake Hazen, Canada	81°08'N	71°04'W	Meadow (wet)	<i>Carex</i> spp., <i>Eriophorum</i> spp.	79 ^b	Emmerton et al. 2016
Longyearbyen, Svalbard	78°11'N	15°55'E	Mixed dry and wet area	<i>Salix polaris</i> , <i>Eriophorum scheuchzeri</i>	82	Pirk et al. 2017
Ny-Ålesund, Svalbard	78°55'N	11°57'E	Polar semi-desert (dry)	<i>Salix polaris</i> , <i>Sanionia uncinata</i>	0	Lüers et al. 2014
Ny-Ålesund, Svalbard	78°55'N	11°57'E	Polar semi-desert (dry)	<i>Saxifraga oppositifolia</i> , <i>Cetraria delisei</i>	9 ^a	Lloyd 2001a
Ny-Ålesund, Svalbard	78°56'N	11°55'E	Heath, snowbed	<i>Saxifraga oppositifolia</i> , <i>Drepanocladus</i> spp.	-5 to 5 ^b	Lloyd 2001b
Ny-Ålesund, Svalbard	78°55'N	11°50'E	Polar semi-desert (dry)	<i>Salix polaris</i> , <i>Sanionia uncinata</i>	2 to 19 ^b	Uchida et al. 2016

^aOne growing season. ^bOne summer season.

The relationships of NPP and NEP in moss tundra with the carbon accumulation rate can be described by the following equations (Nakatsubo et al. 2015):

$$\text{Carbon accumulation} = NPP - R_{\text{peat}} - C_{\text{loss}} \quad (10)$$

$$= NEP - C_{\text{loss}}, \quad (11)$$

where R_{peat} is the peat layer respiration (respiration of the brown layer in this study) and C_{loss} is the carbon loss other than respiratory loss (e.g., leaching) from the peat and dead moss layer. Although CH_4 flux can also contribute to carbon flow, its contribution to total carbon flow is likely negligible at our study site. If the maximum CH_4 efflux rate observed in the field ($65 \mu\text{gCH}_4\text{-C m}^{-2} \text{h}^{-1}$) were sustained throughout one growing season, total CH_4 emissions from the moss tundra would be less than 0.2 gC m^{-2} .

Nakatsubo et al. (2015) estimated the apparent rates of carbon accumulation to be $9.0\text{--}19.2 \text{ (gC m}^{-2} \text{ yr}^{-1})$ based on the ^{14}C age and the amount of peat in the active layer. NEP during the growing season estimated in this study ($67\text{--}88 \text{ gC m}^{-2}$) was much greater than the apparent rates

of carbon accumulation at this study site. This may indicate that a significant proportion of fixed carbon was lost from the peat and dead moss layers as dissolved carbon (C_{loss}). Previous studies have demonstrated that the loss of carbon via organic carbon export is an important component of the carbon balance of northern peatland (Roulet et al. 2007). Although there are cases in which the lateral carbon export is less relevant compared with the vertical carbon fluxes (Beckebanze et al. 2022), Billett et al. (2004) reported that net carbon loss in drainage water, including both the downstream flux and evasion of CO_2 from the stream surface to the atmosphere, was greater than or equal to the net annual carbon uptake stemming from photosynthesis/respiration at the land surface in a lowland temperate peatland catchment. Although no published data are available for Svalbard, a significant proportion of fixed carbon is likely lost through water flow.

Another factor that requires consideration is the recent warming trend. Nordli et al. (2020) reported that the rate of warming since 1991 at Svalbard Airport is $1.7 \text{ }^\circ\text{C/decade}$, which is more than twice the Arctic average and approximately seven times the global average for the same

period. They also reported that the number of days warmer than 0 and 5 °C has increased by 25 (21%) and 22 (59%), respectively, per year compared with that during the 1961–1990 standard normal period for 1991–2018 (Nordli et al. 2020). These changes lengthen the growing season, which affects productivity.

Conclusion

Previous studies have shown that moss tundra plays an important role in carbon sequestration and carbon storage in the High-Arctic terrestrial ecosystem (Rozema et al. 2006; Nakatsubo et al. 2015). Our results indicate that the productivity of moss tundra is high compared with that of other vegetation types in this area, which confirms that moss tundra has a significant effect on regional carbon dynamics.

NEP is currently much larger than the carbon accumulation rates reported for this study site. One possible explanation for the difference between NEP and carbon accumulation is that a significant proportion of fixed carbon is lost from the peat layer. Arctic rivers are known to transport large quantities of organic and inorganic carbon to the Arctic Ocean (Holmes et al. 2008; Loughheed et al. 2020; McGovern et al. 2020). If this is also true for the streams that flow through High-Arctic moss tundra, this pathway may have a significant impact on coastal waters.

The recent warming trend will also likely affect the productivity of moss tundra. Moss tundra is dominated by evergreen perennial plants that have the potential to be photosynthetically active throughout the year; therefore, these plants will likely respond directly to future climate change by increasing their photosynthetic activity.

Acknowledgements

The authors would like to thank Yasuo Iimura (The University of Shiga Prefecture) for assistance with fieldwork. This work is a contribution to the International Arctic Science Committee (IASC) project T-MOSAIC (Terrestrial Multidisciplinary distributed Observatories for the Study of Arctic Connections). We thank Edanz (<https://jp.edanz.com/ac>) for editing the English text of a draft of this manuscript.

Disclosure statement

The authors report no conflict of interest.

Funding

This study was partly supported by Grants-in-Aid for Scientific Research (nos. 20405010, 24405009, 16H05622

and 22H03734) from the Japan Society for the Promotion of Science (JSPS). This study was a contribution to the project ArCS II (Arctic Challenge for Sustainability II, Programme Grant No. JPMXD1420318865) supported by the Ministry of Education, Culture, Sports, Science and Technology, Japan.

References

- Beckeбанze L., Runkle B.R.K., Walz J., Wille C., Holl D., Helbig M., Boike J., Sachs T. & Kutzbach L. 2022. Lateral carbon export has low impact on the net ecosystem carbon balance of a polygonal tundra catchment. *Biogeosciences* 19, 3863–3876, doi: 10.5194/bg-19-3863-2022.
- Billett M.F., Palmer S.M., Hope D., Deacon C., Storeton-West R., Hargreaves K.J., Flechard C. & Fowler D. 2004. Linking land–atmosphere–stream carbon fluxes in a lowland peatland system. *Global Biogeochemical Cycles* 18, GB1024, doi: 10.1029/2003GB002058.
- Emmerton C.A., St. Louis V.L., Humphreys E.R., Gamon J.A., Barker J.D. & Pastorello G.Z. 2016. Net ecosystem exchange of CO₂ with rapidly changing High Arctic landscapes. *Global Change Biology* 22, 1185–1200, doi: 10.1111/gcb.13064.
- Frolking S., Roulet N.T., Moore T.R., Lafleur P.M., Bubier J.L. & Crill P.M. 2002. Modeling seasonal to annual carbon balance of Mer Bleue Bog, Ontario, Canada. *Global Biogeochemical Cycles* 16, article no. 1030, doi: 10.1029/2001GB001457.
- Groendahl L., Friborg T. & Soegaard H. 2007. Temperature and snow-melt controls on interannual variability in carbon exchange in the High Arctic. *Theoretical and Applied Climatology* 88, 111–125, doi: 10.1007/s00704-005-0228-y.
- Harley P.C., Tenhunen J.D., Murray K.J. & Beyers J. 1989. Irradiance and temperature effects on photosynthesis of tussock tundra sphagnum mosses from the foothills of the Philip Smith Mountains, Alaska. *Oecologia* 79, 251–259, doi: 10.1007/BF00388485.
- Hayashi K., Cooper E.J., Loonen M.J.J.E., Kishimoto-Mo A.W., Motohka T., Uchida M. & Nakatsubo T. 2014. Potential role of Svalbard reindeer winter droppings in atmosphere–land exchanges of methane and nitrous oxide during summer. *Polar Science* 8, 196–206, doi: 10.1016/j.polar.2013.11.002.
- Hirota M., Zhang P., Gu S., Shen H., Kuriyama T., Li Y. & Tang Y. 2010. Small-scale variation in ecosystem CO₂ fluxes in an alpine meadow depends on plant biomass and species richness. *Journal of Plant Research* 123, 531–541, doi: 10.1007/s10265-010-0315-8.
- Holmes R.M., McClelland J.W., Raymond P.A., Frazer B.B., Peterson B.J. & Stieglitz M. 2008. Lability of DOC transported by Alaskan rivers to the Arctic Ocean. *Geophysical Research Letters* 35, L03402, doi: 10.1029/2007GL032837.
- IPCC (Intergovernmental Panel on Climate Change) 2021. *Climate change 2021: the physical science basis. Contribution of Working Group I to the sixth assessment report of the Intergovernmental Panel on Climate Change*. V. Masson-Delmotte et al. (eds.). Cambridge: Cambridge University Press.
- Lloyd C. 2001a. On the physical controls of the carbon dioxide balance at a High Arctic site in Svalbard. *Theoretical*

- and *Applied Climatology* 70, 167–182, doi: 10.1007/s007040170013.
- Lloyd C. 2001b. The measurement and modelling of the carbon dioxide exchange at a High Arctic site in Svalbard. *Global Change Biology* 7, 405–426, doi: 10.1046/j.1365-2486.2001.00422.x.
- Longton R.E. 1988. *Biology of polar bryophytes and lichens*. Avon: Cambridge University Press.
- Lougheed V.L., Tweedie C.E., Andresen C.G., Armendariz A.M., Escarzaga S.M. & Tarin G. 2020. Patterns and drivers of carbon dioxide concentrations in aquatic ecosystems of the Arctic coastal tundra. *Global Biogeochemical Cycles* 34, e2020GB006552, doi: 10.1029/2020GB006552.
- Lüers J., Westermann S., Piel K. & Boike J. 2014. Annual CO₂ budget and seasonal CO₂ exchange signals at a High Arctic permafrost site on Spitsbergen, Svalbard archipelago. *Biogeosciences* 11, 6307–6322, doi: 10.5194/bg-11-6307-2014.
- McGovern M., Pavlov A.K., Deininger A., Granskog M.A., Leu E., Søreide J.E. & Poste A.E. 2020. Terrestrial inputs drive seasonality in organic matter and nutrient biogeochemistry in a High Arctic fjord system (Isfjorden, Svalbard). *Frontiers in Marine Science* 7, article no. 542563, doi: 10.3389/fmars.2020.542563.
- Muraoka H., Noda H., Uchida U., Ohtsuka T., Koizumi H. & Nakatsubo T. 2008. Photosynthetic characteristics and biomass distribution of the dominant vascular plant species in a high Arctic tundra ecosystem, Ny-Ålesund, Svalbard: implications for their role in ecosystem carbon gain. *Journal of Plant Research* 121, 137–145, doi: 10.1007/s10265-007-0134-8.
- Muraoka H., Uchida M., Mishio M., Nakatsubo T., Kanda H. & Koizumi H. 2002. Leaf photosynthetic characteristics and net primary production of the polar willow (*Salix polaris*) in a High Arctic polar semi-desert, Ny-Ålesund, Svalbard. *Canadian Journal of Botany* 80, 1193–1202, doi: 10.1139/b02-108.
- Nakatsubo T. 2002. Predicting the impact of climatic warming on the carbon balance of the moss *Sanionia uncinata* on a maritime Antarctic island. *Journal of Plant Research* 115, 99–106, doi: 10.1007/s102650200014.
- Nakatsubo T., Uchida M., Sasaki A., Kondo M., Yoshitake S. & Kanda H. 2015. Carbon accumulation rate of peatland in the High Arctic, Svalbard: implications for carbon sequestration. *Polar Science* 9, 267–275, doi: 10.1016/j.polar.2014.12.002.
- Nordli Ø., Wyszynski P., Gjelten H.M., Isaksen K., Łupikasza E., Niedźwiedz T. & Przybylak R. 2020. Revisiting the extended Svalbard Airport monthly temperature series, and the compiled corresponding daily series 1898–2018. *Polar Research* 39, article no. 3614, doi: 10.33265/polar.v39.3614.
- Opaliński K.W. 1991. Primary production and organic matter destruction in Spitsbergen tundra. *Polish Polar Research* 12, 419–434.
- Pirk N., Sievers J., Mertes J., Parmentier F.-J.W., Mastepanov M. & Christensen T.R. 2017. Spatial variability of CO₂ uptake in polygonal tundra: assessing low-frequency disturbances in eddy covariance flux estimates. *Biogeosciences* 14, 3157–3169, doi: 10.5194/bg-14-3157-2017.
- Roulet N.T., Lafleur P.M., Richard P.J.H., Moore T.R., Humphreys E.R. & Bubier J. 2007. Contemporary carbon balance and late Holocene carbon accumulation in a northern peatland. *Global Change Biology* 13, 397–411, doi: 10.1111/j.1365-2486.2006.01292.x.
- Rozema J., Boelen P., Doorenbosch M., Bohncke S., Blokker P., Boekel C., Broekman R.A. & Konert M. 2006. A vegetation, climate and environment reconstruction based on palynological analyses of High Arctic tundra peat cores (5000–6000 years BP) from Svalbard. *Plant Ecology* 182, 155–173, doi: 10.1007/s11258-005-9024-0.
- Tveit A., Schwacke R., Svenning M. & Urich T. 2013. Organic carbon transformations in High-Arctic peat soils: key functions and microorganisms. *The ISME Journal* 7, 299–311, doi: 10.1038/ismej.2012.99.
- Uchida M., Kishimoto A., Muraoka H., Nakatsubo T., Kanda H. & Koizumi H. 2010. Seasonal shift in factors controlling net ecosystem production in a High Arctic terrestrial ecosystem. *Journal of Plant Research* 123, 79–85, doi: 10.1007/s10265-009-0260-6.
- Uchida M., Muraoka H. & Nakatsubo T. 2016. Sensitivity analysis of ecosystem CO₂ exchange to climate change in High Arctic tundra using an ecological process-based model. *Polar Biology* 39, 251–265, doi: 10.1007/s00300-015-1777-x.
- Uchida M., Muraoka H., Nakatsubo T., Bekku Y., Ueno T., Kanda H. & Koizumi H. 2002. Net photosynthesis, respiration, and production of the moss *Sanionia uncinata* on a glacier foreland in the High Arctic, Ny-Ålesund, Svalbard. *Arctic, Antarctic, and Alpine Research* 34, 287–292, doi: 10.1080/15230430.2002.12003496.
- Uchida M., Nakatsubo T., Kanda H. & Koizumi H. 2006. Estimation of the annual primary production of the lichen *Cetrariella delisei* in a glacier foreland in the High Arctic, Ny-Ålesund, Svalbard. *Polar Research* 25, 39–49, doi: 10.3402/polar.v25i1.6237.
- Vanderpuy A.W., Elvebakk A. & Nilssen L. 2002. Plant communities along environmental gradients of High-Arctic mires in Sassendalen, Svalbard. *Journal of Vegetation Science* 13, 875–884, doi: 10.1111/j.1654-1103.2002.tb02117.x.
- Welker J.M., Fahnestock J.T., Henry G.H.R., O’Dea K.W. & Chimner R.A. 2004. CO₂ exchange in three Canadian High Arctic ecosystems: response to long-term experimental warming. *Global Change Biology* 10, 1981–1995, doi: 10.1111/j.1365-2486.2004.00857.x.
- Yoshitake S., Uchida M., Koizumi H., Kanda H. & Nakatsubo T. 2010. Production of biological soil crusts in the early stage of primary succession on a High Arctic glacier foreland. *New Phytologist* 186, 451–460, doi: 10.1111/j.1469-8137.2010.03180.x.
- Yoshitake S., Uchida M., Ohtsuka T., Kanda H., Koizumi H. & Nakatsubo T. 2011. Vegetation development and carbon storage on a glacier foreland in the High Arctic, Ny-Ålesund, Svalbard. *Polar Science* 5, 391–397, doi: 10.1016/j.polar.2011.03.002.
- Yr 2021. Ny-Ålesund. (Weather data.) Accessed on the internet at <https://www.yr.no/en/statistics/graph/5-99910/Norway/Svalbard/Svalbard/Ny-Ålesund> on 24 May 2021

Yu Z.C. 2012. Northern peat land carbon stocks and dynamics: a review. *Biogeosciences* 9, 4071–4085, doi: 10.5194/bg-9-4071-2012.

Zhang W., Jansson P.-E., Schurgers G., Hollesen J., Lund M., Abermann J. & Elberling B. 2018. Process-oriented

modeling of a High Arctic tundra ecosystem: long-term carbon budget and ecosystem responses to inter-annual variations of climate. *Journal of Geophysical Research—Biogeosciences* 123, 1178–1196, doi: 10.1002/2017JG003956.